www.czasopisma.pan.pl PAN POLSKA AKADEMIA NAUK www.journals.pan.pl

Arch. Metall. Mater. **67** (2022), 3, 1007-1020

DOI: https://doi.org/10.24425/amm.2022.139695

A. KODENTSOV[1*], C. CSERHÁTI[2]

GASEOUS NITRIDING OF BINARY Ni-Cr ALLOYS – OBSERVATION AND INTERPRETATION OF MICROSTRUCTURAL FEATURES

Gaseous nitriding of binary Ni-Cr solid-solution alloys was studied at 1125ºC over the range 1 to 6000 bar of N_2-pressure. At the specified temperature the nitriding response of the Ni-Cr alloys depends on the Cr-content in the initial alloy and activity (fugacity) of nitrogen at the gas/metal interface. Transition from cubic δ-CrN to hexagonal β-Cr_2N precipitation occurs within the reaction zone after nitrogenization at 1125ºC under nitrogen pressure 100-6000 bar when chromium content in the initial alloy is 28 at. % or higher. It was found that a ternary phase, π ($Cr_{12.8}Ni_{7.2}N_{4.0}$) is formed inside the Ni32Cr alloy upon cooling in nitrogen after nitriding at 1125ºC and 1 bar of N_2. Experimental evidence is presented that π-phase is involved in peritectoid relations with β-Cr_2N and γ-(Ni-Cr) solid solution. It was also demonstrated that nitriding behaviour of the Ni-Cr alloy can be rationalized using pertinent phase diagram information, but, in some cases, effect of mechanical stresses induced upon the internal precipitation can vitiate this prediction.

Keywords: nitridation; Ni-Cr-N system; diffusion; internal precipitation; microstructure

1. Introduction

The present investigation is a part of our continuing research into multi-phase diffusion and reactive phase formation in non-ionic inorganic solids [1,2]. Among a large variety of diffusion-controlled solid-state reactions, internal precipitation in metallic systems is perhaps, one of the most fascinating reaction phenomena. In this paper we shall be concerned with internal nitridation of binary Ni-Cr alloys. It is of particular interest here to take a close look at microstructural evolution of the reaction zone developed during gaseous nitriding of the Ni-Cr solid solutions.

The choice of the nitriding reactions for studying microstructural aspects of the internal precipitation in alloy systems was dictated mainly by the fact that contrary to the interactions involving other penetrating species, like for example, oxygen, carbon, or sulfur, nitridation experiments can be performed under a wide range of well-defined oxidant (nitrogen) activities imposed on the external metal surface [1].

The binary Ni-Cr alloys were selected for the nitriding experiments based on several reasons. Phase diagram of the Ni-Cr system is simple eutectic with an ordering reaction at low temperature (<590ºC) around the composition "Ni_2Cr" and an extensive solid-state solubility of chromium in nickel (up to ~50 at. %) at the eutectic temperature 1345ºC [3]. Solubility of nitrogen in solid nickel is negligible and no nitride phases exist in the Ni-N system above 600ºC [4]. On the other hand, two nitrides, viz. cubic δ-CrN (*cP*8; $Fm\bar{3}m$) and hexagonal β-Cr_2N (*hP*9; $P\bar{3}1m$) are stable in the binary Cr-N system [5]. (Note. Both nitrides have narrow region of homogeneity, but hereafter, these intermediate phases will be denoted in their binary formulae.) Therefore, one might expect that depending upon nitrogenizing conditions, i.e., external nitrogen fugacity, temperature, and the solute (Cr) content in the alloy used, one or both nitrides may form in the reaction zone. The relative simplicity of the ternary Ni-Cr-N system gives an opportunity to perform a comparative study of nitriding behaviour of Ni-Cr solid-solution (γ) alloys under various experimental conditions. Results of such nitridation experiments with the binary Ni-Cr alloys are relatively easy to interpret, and microstructure of the product reaction zones lends themselves to a rather straightforward analysis, and therefore, it may serve as a model for other internal precipitation reactions in the solid-state.

Reactions of internal precipitation are not only of an academic interest. The internal nitriding of Ni-Cr alloys remains a subject of substantial technological importance, because these

[1] MAT-TECH BV, DEVELOPMENT & TESTING, SON, THE NETHERLANDS
[2] UNIVERSITY OF DEBRECEN HUNGARY FACULTY OF SCIENCES AND TECHNOLOGY, DEPARTMENT OF SOLID STATE PHYSICS, HUNGARY
* Corresponding author: A.Kodentsov@mat-tech.com

© 2022. The Author(s). This is an open-access article distributed under the terms of the Creative Commons Attribution-NonCommercial License (CC BY-NC 4.0, https://creativecommons.org/licenses/by-nc/4.0/deed.en which permits the use, redistribution of the material in any medium or format, transforming and building upon the material, provided that the article is properly cited, the use is noncommercial, and no modifications or adaptations are made.

alloys constitute a base for a number of important corrosion-resistant materials, and the formation of internal nitride precipitates may cause degradation of mechanical properties and even premature failure of high-temperature components. Furthermore, a significant volume increase, accompanying precipitation reactions and low thermal expansion of the nitrides as compared with the metallic alloy matrix result in the generation of stresses which may lead to the formation of microcracks and embrittlement of the near-surface layer [6].

The first paper about nitridation of binary Ni-Cr alloys was published by Rubly and Douglass back in 1991 [7]. The authors conducted a series of experiments in an ammonia+hydrogen mixture over the temperature range 700-900ºC using alloys containing 10-50 wt. % of Cr. Somewhat later, several issues related to thermodynamic, kinetic, and mechanical aspects of internal nitridation reactions have been raised in our publications as well [8-10].

The present article will seek to convey some of the new experimental observations in the nitriding behaviour of binary Ni-Cr solid-solution alloys in nitrogen atmosphere with various pressures ranging from 1 to 6000 bar at 1125ºC and to explain microstructural features of the reaction zone generated in the alloys during nitrogenization under these conditions. Here, we shall be only concerned with nitridation reactions in semi-infinite samples. The latter implies that after the interaction completed, there exists an unreacted domain of the sample, which still retains the initial alloy composition. It is believed that this work will contribute to further understanding of internal precipitation reactions in the solid-state.

2. Experimental details

Throughout the investigation six binary Ni-Cr alloys with nominal Cr-content 5, 10, 15, 22, 28 and 32 at. %, were used in the nitridation experiments. The compositions of the Ni-Cr alloys studied in the present work were in the solid-solution range [3]. (Hereafter, these alloys will be referred to as Ni5Cr, Ni10Cr, etc.).

High-purity metals Ni (99.98%) and Cr (99.95%) were supplied by Goodfellow (UK). The alloys were prepared by melting the constituent metals in arc-furnace under argon atmosphere using a non-consumable tungsten electrode. The weight loss of the alloys after melting was less than 0.5 wt. % relative. The ingots were cold-rolled to a thickness of 1.5 mm. Alloy coupons with dimensions of 8 × 8 mm were cut from the sheets and homogenized at 900ºC for 100 hours under 1 bar of gas-mixture Ar + 10 vol.% H_2 (H_2O < 5 ppm). The grain size of the alloys after this heat-treatment was in the range 100-150 μm. Prior to the nitriding experiments, the surface of the alloy coupons was electropolished and ultrasonically cleaned in acetone.

Nitriding of the alloys at 1 bar of nitrogen was conducted in a vacuum furnace equipped with a gas-inlet system. If quenching of the samples was necessary, a horizontal tube furnace with flowing nitrogen was used. In the experiments performed at 1 bar of nitrogen pressure, the temperature was controlled with an accuracy of ±2 degrees.

For nitriding at 1125ºC and nitrogen pressure of 100 bar, a sintering furnace (KCE, Germany) was employed. In this case, the temperature control was carried out with an optical pyrometer with an accuracy of ±5 degrees.

Nitridation at 900 and 6000 bar of N_2-pressure were performed in an ultra-high pressure furnace made by UNIPRESS (Poland). The nitrogen pressure was controlled by using a manganine gauge within ±10 bar accuracy. Temperature control was carried out within ±3 degrees accuracy. More technical details about the ultra-high pressure equipment can be found elsewhere [11].

All nitriding experiments were conducted in pure nitrogen (O_2 < 5 ppm; H_2O < 5 ppm). Before the nitriding run under isostatic conditions, the furnaces were evacuated up to 10^{-4} mbar, filled with pure nitrogen and evacuated again. After nitridation under these conditions no oxide formation was detected at the surface of the samples with the analytical techniques used in the present work.

The surface of the alloys after nitriding, was examined by X-ray diffraction analysis (XRD) with a cylindrical texture camera using a Ni-filtered Cu$K\alpha$ radiation [12]. Then, the nitrided samples were cross-sectioned and after standard metallographic preparation were investigated, first, by optical microscopy, and then by Scanning Electron Microscopy (SEM) and Electron Probe Microanalysis (EPMA).

Microstructure of the reaction zones was also investigated with Transmission Electron Microscopy (TEM) and electron diffraction. Plan-view and cross-sectional specimens taken from the nitrided samples were prepared by mechanical thinning and dimple grinding; electron beam transparency was accomplished by 6 kV argon-ion milling.

3. Results: Diversity of forms and variations of microstructures generated in binary Ni-Cr solid-solution alloys by reaction with N_2-gas

3.1. Nitridation of Ni-Cr alloy under external N_2-pressure of 1 bar

Only hexagonal nitride β-Cr_2N was detected at the surface and inside the Ni-Cr alloys with Cr-content 28 and 32 at. % after annealing at 1125ºC under 1 bar of nitrogen and subsequent quenching in cold water, while no superficial nitride formation was detected in all alloys with lower (≤22 at. %) Cr-contents used in the present investigation. Typical morphology of the reaction zone developed in a Ni 32Cr alloy during nitridation under these conditions for 16 hours is shown in Fig. 1.

The rection product consists of both a superficial nitride layer and nitride precipitates inside the alloy, with the surface layer being separated from the internal precipitation zone by a layer of Ni-Cr solid-solution devoid of any precipitates. Transmission Electron Microscopy (TEM) and electron diffrac-

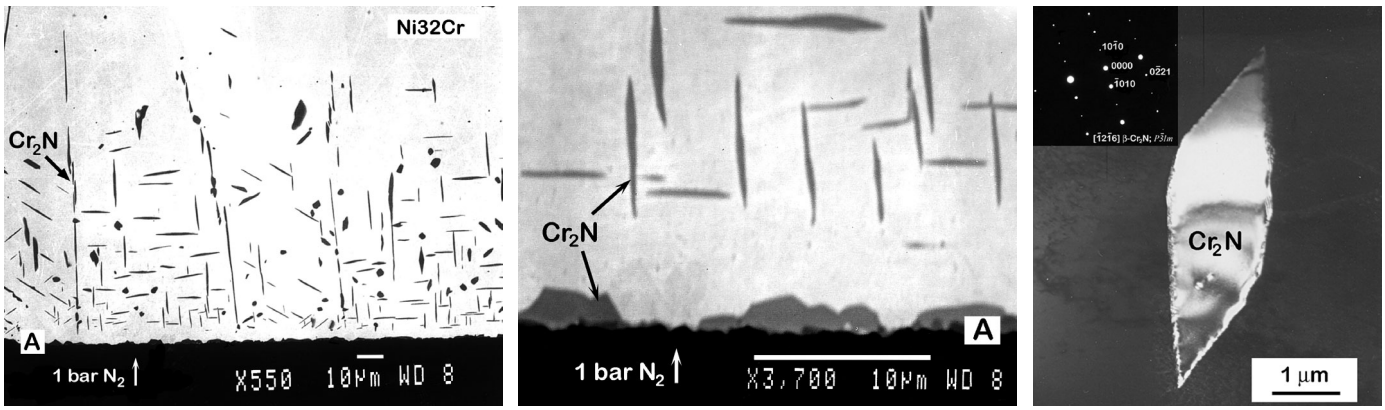

a) b) c)

Fig. 1. Backscattered Electron Images (BEIs) of the reaction zone developed in a Ni32Cr after nitriding under 1 bar of N_2 at 1125ºC for 16 hours and quenching in water: a) general view and b) magnified area showing formation of the surface nitride; c) dark-field (DF) TEM image of the precipitate taken with a $0\bar{2}21$ spot in the Selected Area Electron Diffraction Pattern (SAED) shown in the insert, which was obtained from the internal nitride particle and indexed as $[\bar{1}2\bar{1}6]$ direction in the hexagonal lattice of β-Cr_2N (*hP*9; $P\bar{3}1m$; $a = 0.4811$ nm, $c = 0.4484$ nm [13]. (Letter A indicates the location of the gas/metal interface.)

tion verified that under experimental conditions used, internal precipitation of hexagonal (*hP*9) dichromate nitride, β-Cr_2N takes place inside the γ-Ni-Cr solid-solution matrix (Fig. 1c).

From the micrographs shown in Figs. 1a, b, one can see that the internal nitrogenization process in this sample favors a "needle"-type morphology of the precipitates. However, it is likely that what appeared to be needles in these images are actually seen to be platelets standing on edge. It is also to be noticed that there appears to be some preferred crystallographic planes in the alloy matrix, on which these plate-like nitride precipitates form and grow, which is manifested by the consistent angles found between the platelets.

When in nitriding experiments at 1 bar of N_2-gas, cooling from the annealing temperature 1125ºC was performed under 1 bar of nitrogen pressure, but at significantly lower rate, at about 300 degrees/ hour, the formation of superficial β-Cr_2N and ternary phase of the Ni-Cr-N system deep inside the nitride zone was observed (Fig. 2).

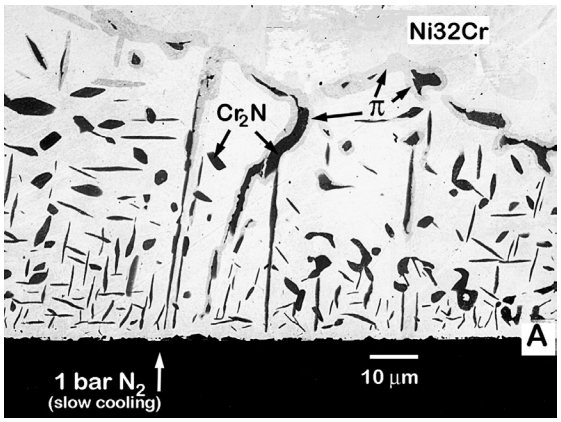

Fig. 2. The formation of the ternary π-phase of the Ni-Cr-N system in a Ni-Cr alloy with 32 at. % Cr after nitriding at 1125ºC and 1 bar of N_2 for 16 hours and cooling under 1 bar of nitrogen at the rate of ~300 degrees/hour (BEI). (Letter A indicates the position of the gas/metal interface.)

Using EPMA, composition of this ternary phase was determined as $Cr_{12.8}Ni_{7.2}N_{4.0}$. Probably, this ternary phase is the same nitride phase that reported by Ono et al. [14] and designated as a π-phase.

3.2. Nitriding response of Ni-Cr alloys to nitrogen atmosphere with pressure of 100 bar at 1125ºC

No nitride phases were detected in a Ni5Cr alloy after exposure at 1125ºC to 100 bar of Nitrogen, but after nitriding of a Ni10Cr alloy under the same conditions, cubic δ-CrN was detected at the alloy surface by XRD analysis, and electron diffraction confirmed the formation of internal precipitates of the same nitride (cubic CrN) also inside the alloy as matrix (Fig. 3).

Also observed is that under these experimental circumstances, nitriding behaviour of the alloys with the Cr-content up to 22 at. %, is very similar. However, the increase of Cr-concentration in the initial solid solution above 28 at. %, leads to the formation of a superficial layer of cubic nitride δ-CrN, and underneath of the external layer, internal precipitates of another binary nitride, i.e., hexagonal β-Cr_2N, are formed. As an example, a typical reaction zone morphology developed in Ni32Cr alloy during nitriding at 1125ºC and 100 bar of N_2-pressure is given in Fig. 4.

The formation of cubic δ-CrN on the alloy surface was verified by XRD analysis with a cylindrical texture camera, and electron diffraction gave positive identification for the precipitation of hexagonal β-Cr_2N in the central part of the internally nitrided zone (Figs. 4c, d). (Note. In the XRD pattern given in Fig. 4c, the strong intensity modulation of the diffraction lines originated from the Ni-Cr substrate are due to the coarse grain structure of the alloy (grain size >100 µm)).

However, at the "corners" of the nitride sample, the formation of both δ-CrN- and ε-Cr_2N-precipitates was observed (Fig. 4b). The average concentration of chromium in the γ-Ni-

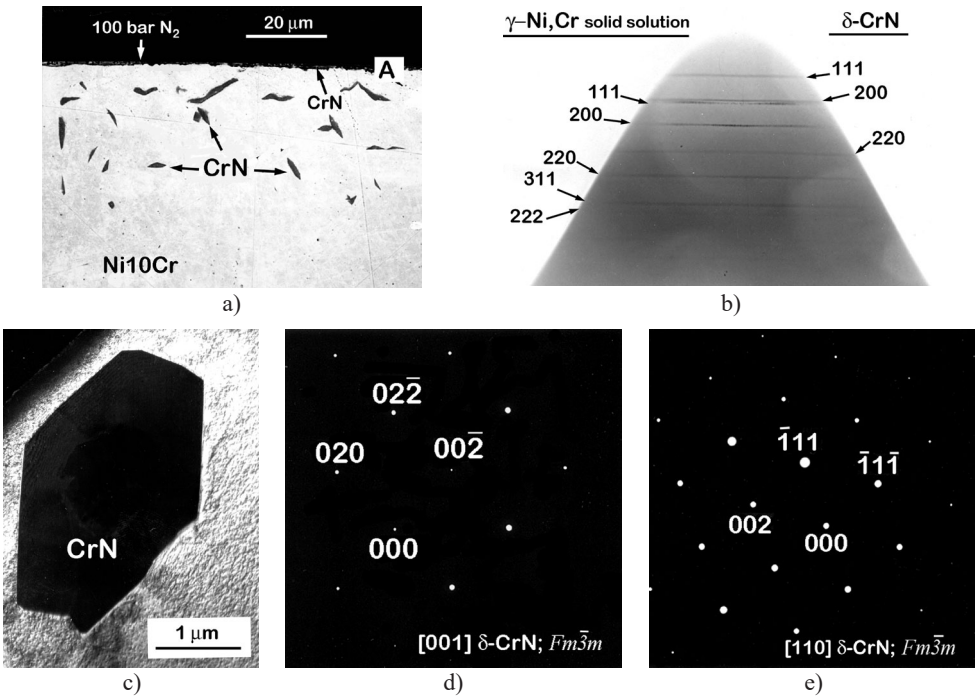

a) b) c) d) e)

Fig. 3. The formation of cubic δ-CrN in Ni10Cr alloy during nitriding at 1125ºC and 100 bar of N_2-pressure for 4 hours: a) Secondary Electron Image (SEI) of the reaction zone (A indicates the position of the gas/metal interface); b) XRD pattern taken from the surface of the nitrided alloy with a cylindrical texture camera using Ni-filtered Cu$K\alpha$ radiation (A number of diffraction lines of Ni-Cr solid solution and δ-CrN can be identified by comparing their d-spacing values calculated with data given in [3] and those listed in [15]); c) bright-field (BF) TEM image of the internal nitride particle along with d) and e) Selected Area Electron Diffraction (SAED) patterns obtained from the precipitate and indexed as [001] and [110] directions in the cubic lattice of δ-CrN ($Fm\bar{3}m$; a = 4148 nm [15])

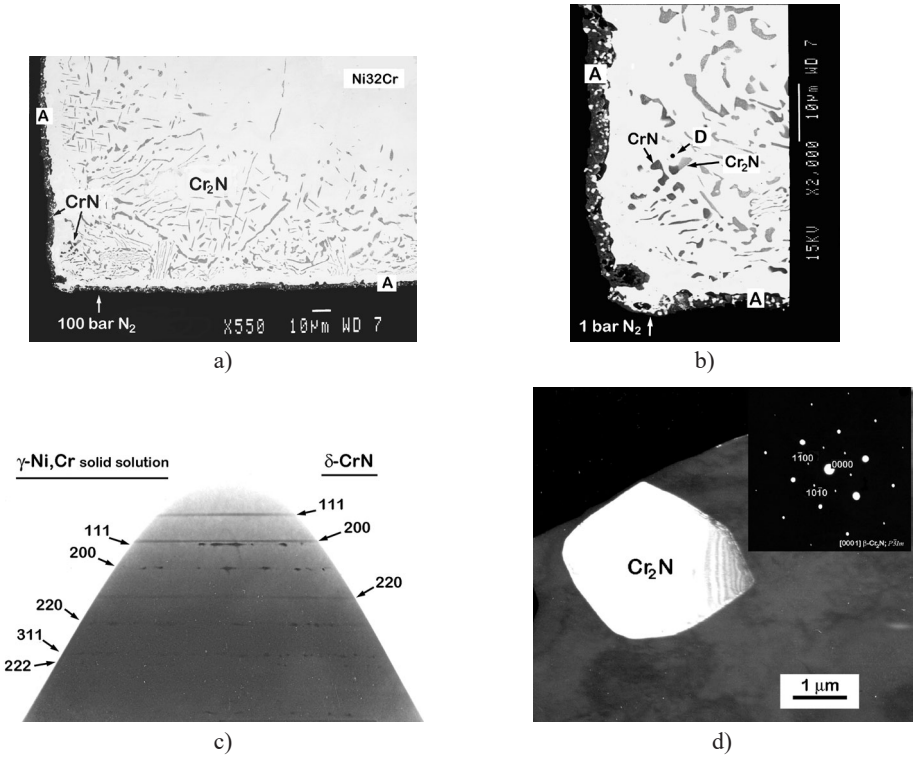

a) b) c) d)

Fig. 4. Backscattered Electron Images (BEIs) of the reaction zone developed during nitriding of Ni32Cr alloy at 1125ºC under 100 bar of N_2-pressure for 4 hours: a) general view and b) magnified image of the sample corner showing formation of the internal precipitates of δ-CrN (Letter A indicates the gas/metal interface); c) XRD pattern taken from the nitrided alloy surface with a cylindrical texture camera using Ni-filtered Cu$K\alpha$ radiation (A number of diffraction lines of Ni-Cr solid solution and δ-CrN can be identified by comparing their d-spacing values calculated with data given in [3] and those listed in [15]) and d) dark-field (DF) TEM image of the precipitate obtained with a $10\bar{1}0$ spot in the Selected Area Electron Diffraction Pattern shown in the insert. The SAED was recorded from the internal nitride particle in the specimen taken from the central part of the reaction zone and indexed as [0001] direction in the hexagonal lattice of β-Cr_2N ($hP9$; $P\bar{3}1m$; a = 0.4811 nm, c = 4484 nm [13])

Cr solid solution, which in equilibrium with both δ-CrN and ε-Cr_2N was determined (in terms of EPMA) as 23.8 ± 0.3 at. % (Point D in Fig. 4b).

Again, as in the case of nitriding at 1 bar of nitrogen, a precipitate-free zone of Ni-Cr based solid-solution matrix between the layer of surface nitride and the region of internal precipitation is discernible within the reaction zone microstructure (Figs. 4a, b).

3.3. Pattern of nitriding behaviour in the Ni-Cr alloy – Nitrogen system at 1125ºC and 900 bar of N_2 – pressure

With increasing external N_2-pressure up to 900 bar, exclusive internal nitridation in the absence of surface nitride layer was found to occur in the alloy with 5 at. % of Cr (Fig. 5a). The internal precipitates have grown large enough to give discrete Selected Area Electron Diffraction (SAED) patterns, and electron diffraction confirmed the formation of cubic δ-CrN during the nitrogenization process (Fig. 5c). One can see that the internal nitridation zone consists of numerous isolated precipitates of cubic δ-CrN with some orientation relationship to the γ-(Ni-Cr) solid-solution matrix phase (Fig. 5a).

Under nitriding conditions used, the formation of surface layer of cubic δ-CrN in combination with internal CrN-precipitates was also found in the alloys with higher Cr-content, like for example, in the Ni22Cr, the nitrided zone microstructure of which, is given in Fig. 6.

It is to be noticed that in this case, the same nitride, i.e., δ-CrN, is formed in both, in the external layer and in the alloy as matrix, which is in contradistinction to the pattern of reaction products developed in the Ni32Cr alloy upon nitriding at the same temperature, but at lower pressure of nitrogen, namely, 100 bar (cf. Fig. 4a).

Quite large particles of CrN can be seen near the precipitate-free zone, while deeper in the alloy, the reaction zone consists of nitride precipitates inside the grains as well as along grain

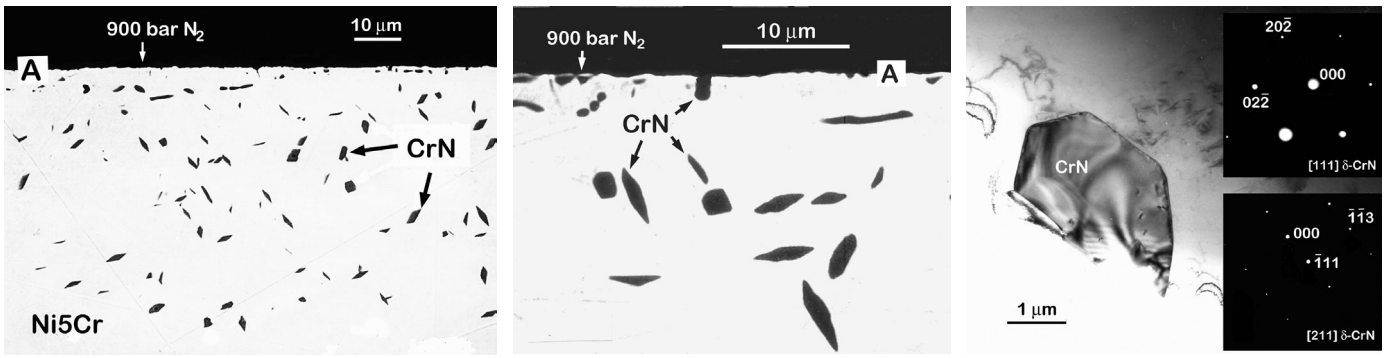

a) d) c)

Fig. 5. Secondary Electron Images (SEI) of the nitrided zone in the Ni5Cr alloy after reaction at 1125ºC for 4 hours under 900 bar of external N_2-pressure: a) general view; b) magnified area in the vicinity of the metal/gas interface and c) bright-field (BF) electron image of the internal nitride precipitate together with Selected Area Electron Diffraction (SAED) patterns (inserts) recorded from the precipitate and indexed as [111] and [211] directions in the cubic lattice of δ-CrN ($Fm\bar{3}m$; a = 4148 nm [15]). (Letter A indicates the locations of the gas/metal interface.)

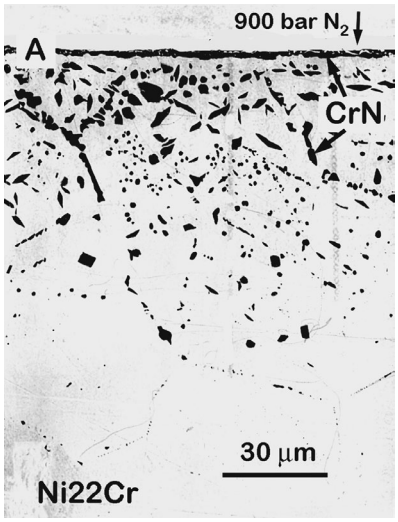

Fig. 6. Reaction zone morphology developed during nitriding at 1125ºC and 900 bar of N_2-pressure for 4 hours in Ni22Cr alloy (SEI) (Letter A indicates the location of the gas/metal interface.)

boundaries of the Ni-Cr alloy matrix. Precipitation along grain boundaries was found even beyond the internal nitridation front.

When Cr-content in the initial alloy was increase to 28 at. %, the formation of both binary nitrides (cubic δ-CrN and hexagonal β-Cr_2N) was observed inside the reaction zone (Fig. 7). One can see that nitridation under these conditions results in reaction zone morphology consisting of an external (superficial) CrN-layer (scale), subsurface zone devoid of precipitates, and zone of internal nitride precipitation. However, contrary to the observations described above for the experiments at 100 bar of external N_2- pressure (Fig. 4), in the present case, the transition from δ-CrN to ε-Cr_2N was found to take place along the entire internally nitrided zone. Using EPMA, the concentration of chromium in the γ-(Ni-Cr) solid-solution which is in equilibrium with both δ-CrN- and ε-Cr_2N-precipitates (e.g., Point D in Fig. 7c) was determined as 24.2 ± 0.5 at. %. It should be noted that this value is very close to that measured for in the γ-Ni-Cr solid solution equilibrated with both binary nitride phases, δ-CrN and ε-Cr_2N

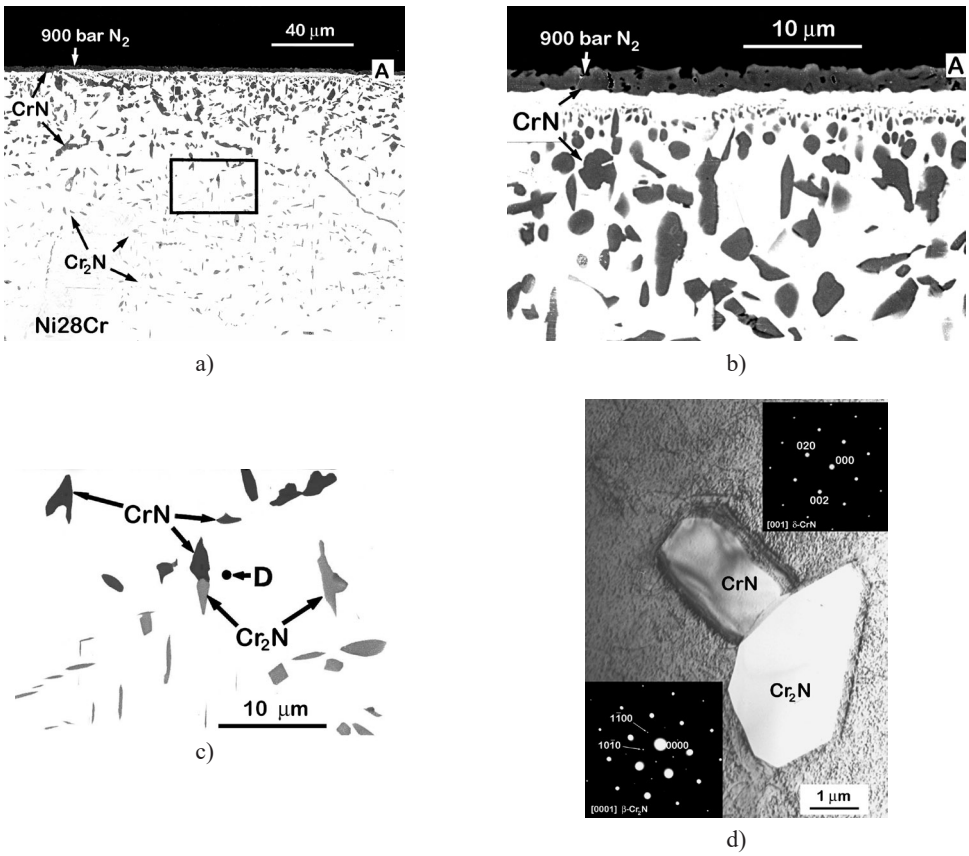

Fig. 7. Microstructure of the reaction zone developed in Ni28Cr alloy during nitriding at 1125ºC and 900 bar of N_2-pressure for 4 hours (BEIs): a) general view; b) magnified domain in the vicinity of the metal/gas interface and c) zoomed area outlined by rectangle in (b) together with d) bright-field (BF) electron image showing contiguous nitride precipitates along with Selected Area Electron Diffraction (SAED) patterns (inserts) taken from the internal nitride particles verifying the transition from cubic δ-CrN to hexagonal β-Cr_2N precipitation within the reaction zone. (Letter A indicates the location of the gas/metal interface.)

inside the reaction zone developed in the Ni32Cr alloy during nitrogenization at the same temperature, but at significantly lower external nitrogen pressure (Point D in Fig. 4b).

In some domains of the internally nitride zone, grain-boundary precipitation is evident, along with a slight denuding effect immediately adjacent, which is manifested as a lower density of precipitates. The reaction front in the nitrided samples was nonplanar, and therefore, attempts to study kinetics of the nitridation zone growth were inconclusive.

One common morphological feature of the reaction zones, which should be noticed from the Figs. 6 and 7 a, b is the presence of a precipitate-free layer of the γ-(Ni-Cr) solid solution between the superficial nitride scale and the zone of internal precipitation. Similar observation has been already described above for the case of the reaction zone developed in the Ni32Cr alloy upon nitriding at 1125ºC and 100 bar of nitrogen pressure (Figs. 4a and 4b).

3.4. Reaction zone morphology developed in Ni-Cr solid-solution alloys during nitrogenization at 1125ºC under 6000 bar of N_2-pressure

When nitrogen pressure of 6000 bar was applied upon the system, the formation of only internal nitride precipitates in the absence of superficial nitride layer was observed after interaction at 1125ºC in all alloy compositions tested in the present investigation. Typical reaction zone microstructures developed in the Ni-Cr alloys containing 5-15 at. % of Cr during nitrogenization under these conditions for 4 hours are shown in a series of images given in Fig. 8 and Fig. 9. (Note. For visual appreciation, the micrographs showing general views of the nitride zones have been arranged in these figures in the order of increasing concentration of solute element (Cr) in the initial Ni-Cr solid-solution alloy.)

Individual precipitates in the vicinity of metal/gas contact surface formed upon nitriding of Ni5Cr alloy were very fine and hardly resolvable by SEM. Therefore, microstructure of this part of the rection zone was studied with TEM. A bright-field electron image of the nitrided zone recorded from the specimen taken in the vicinity of the metal-gas interface shows that precipitates are generally rounded and have dimensions in order of 100 nm (Fig. 8c), and electron diffraction confirmed the formation of cubic δ-CrN during nitrogenization process.

One can see that reaction product morphologies in these three samples are broadly similar. The internally nitride zones have a “dual-layer” (“duplex”) appearance. Precipitates within the “sub-layer” adjoined to the alloy surface are small and generally rounded, becoming coarser with increasing depth,

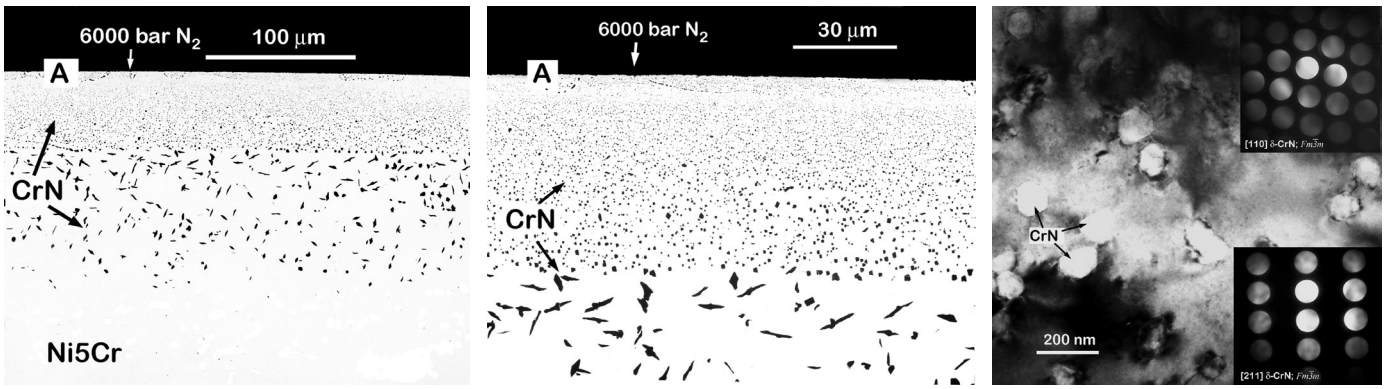

a) b) c)

Fig. 8. Backscattered Electron Images (BEIs) of the nitrided zone developed in a Ni5Cr alloy after annealing at 1125ºC and 6000 bar of N_2 for 4 hours: a) general views; b) zoomed area of the reaction zone showing transition from rounded to plate-like precipitate morphology (Letter A indicates the location of the gas/metal interface) and c) bright-field (BF) electron image of the precipitation zone taken in the vicinity of the metal-gas interface together with Convergent Beam Electron Diffraction (CBED) patterns (inserts) obtained from the internal precipitate verifying the formation of cubic chromium nitride during nitridation

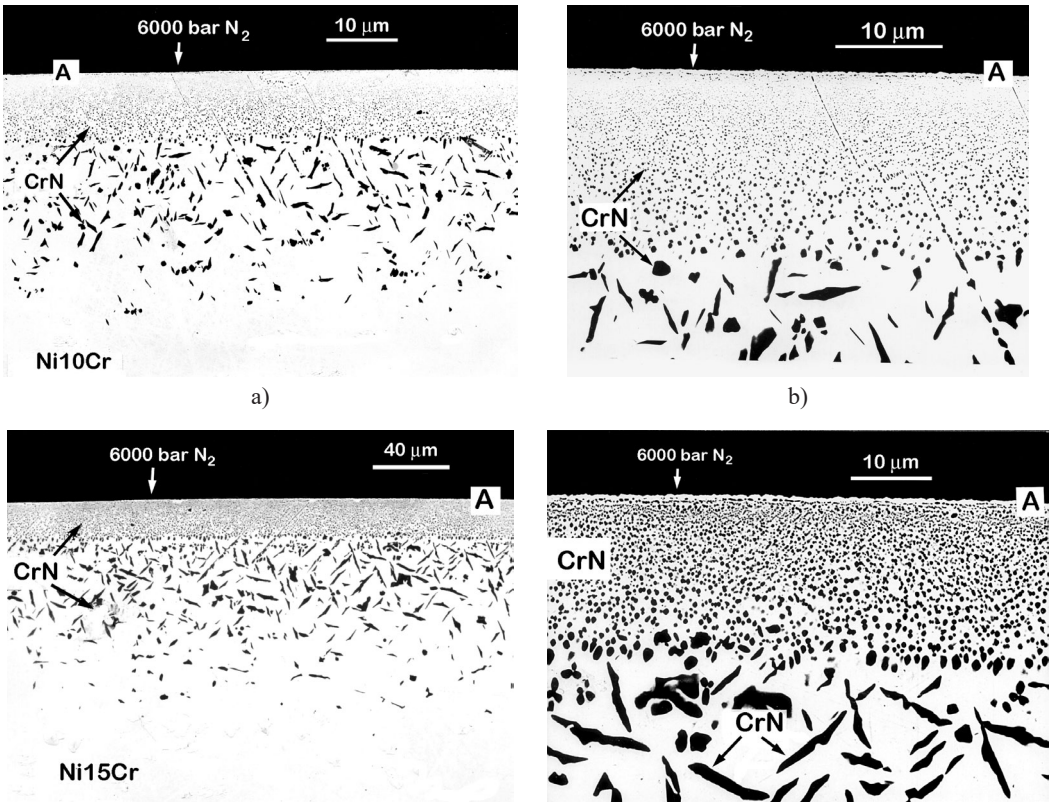

a) b) c) d)

Fig. 9. Backscattered Electron Images (BEIs) of the nitrided zone in Ni10Cr and Ni15Cr alloys after annealing at 1125ºC and 6000 bar of N_2 for 4 hours: a), c) general views and b), d) magnified areas of the reaction zones showing transition from rounded to plate-like precipitate morphology. (Letter A indicates the location of the gas/metal interface.)

and at certain distance from the gas/metal interface, the nitride precipitates favor a plate-like morphology, with some orientation relationship to the g-(Ni-based) solid solution matrix. It is also interesting to remark, in this context, that microstructure of the sub-layer containing plate-like particles is superficially similar to that developed in Ni5Cr alloy during nitriding at the same temperature, but under significantly lower external nitrogen pressure, namely, 900 bar (cf. Fig. 5a).

It is to be noted that variation in number density and size of precipitates through the sub-layer composing of rounded CrN-inclusions changes with changing the initial alloy composition, and thickness of this sub-layer as well as its relative width within the internally nitride zone decreases with increasing Cr-content in the original γ-(Ni-Cr) solid solution. The internal precipitation front was not flat, and limited attempts to analyze growth kinetics of the internally nitridated zone proved unsuccessful.

One more microstructural feature is to be mentioned here. Close inspection of the reaction zone immediately below gas/metal contact surface revealed the presence a metallic layer devoid of any nitride precipitates. This can be appreciated just by looking at the back-scattered electron image given in Figs. 9b, d. Although rather thin, but continuous, precipitate-free metallic layer is clear visible on the alloy surface.

A surprizing experimental fact is the observation that no superficial nitride formation takes place in Ni-Cr alloys with higher (up to 32 at. %) Cr-content after interaction at 1125ºC with N_2-gas under pressure of 6000 bar. The reaction product consists of exclusively internal nitride precipitates inside a solid-solution matrix. A series of backscattered electron images illustrating the most prominent microstructural features of the reaction zone generated in a Ni28Cr alloy during nitriding under these experimental conditions is presented in Fig. 10 as an example.

Relatively small, rather equiaxial precipitates of cubic CrN were formed close to the gas/alloy interface and the increase in size of these nitride particles with depth below the specimen surface can be clearly seen. Deeper in the alloy, precipitates become even coarser and transformed to a "Widmanstätten"-type structure of relatively large, angular precipitates. In some areas of the precipitation zone, intergranular nitride formation with plate-like particles inside of grains was observed.

At still greater depth below the alloy surface, precipitates of hexagonal β-Cr_2N were detected. Again, as in the case of the nitriding of this alloy at 900 bar of N_2-pressure, the transition from CrN- to Cr_2N-precipitation is discernible along the entire nitride zone (Figs. 10a, c). In some domains of the internal precipitation zone, this transition also occurs at grain boundaries (Fig. 10c).

The Cr-content in the γ-(Ni-Cr) based solid solution equilibrated with both nitrides was found (with EPMA) to be 24.3 ± 0.3 at. % (Point D in Fig. 10c), which is very close to the values measured in the γ-(Ni-Cr) based matrix at the location where transition from the CrN- to Cr_2N-precipitation occurs inside the internally nitride zone of the Ni32Cr and Ni28Cr alloys after annealing at 1125ºC under 100 and 900 bar, respectively (Figs. 4b and 7c). As in the previous cases, the internal nitridation boundary was not sharp, which made it difficult to get reliable kinetic data.

Another interesting morphological feature of the nitride zone is apparent from the microstructure shown in Fig. 10b. As in the alloys with lower Cr-content, a metallic layer denuded of nitride particles was formed on the alloy surface during internal precipitation reaction.

4. Discussion: Phase constitution of the reaction zones generated in binary Ni-Cr solid-solution alloys during gaseous nitriding

Nitriding behaviour of Ni-Cr alloys at specified temperature was observed to change remarkedly with Cr-content in the initial solid-solution alloy and activity (fugacity) of nitrogen at the gas/metal interface. It is also clear that at the temperature of the present nitridation experiments, there is (depending on the fugacity of nitrogen at the alloy surface) a wide variation in morphology of precipitates within the internally nitrided zone for a given alloy with respect to their size, shape, and number density.

It is to be recalled, at this point, that a rigorous treatment of gas-metal reactions, including internal precipitation in alloys, is possible (as in the case of any solid-state reaction [16]) only under assumption that local thermodynamic equilibrium prevails in the reaction zone. The assumption that local equilibrium is established and maintained in the diffusion zone means that diffusion is very slow compared with the rate of reaction to form a new product, i.e., overall kinetics of the process is a diffusion-controlled. (Note. In the case of internal precipitation reactions, this assumption also eliminates the need to consider nucleation and growth of the precipitates on a local scale.)

If, on the other hand, local thermodynamic equilibrium in solid non-equilibrium system is not attained, the quantitative description of the internal precipitation reactions is very difficult. In such a case, instead of applying phenomenological theories, one has to explain an infinite number of situations, all for their own.

In the case of gaseous nitriding, the assumption of attaining local equilibria in the system also implies that uptake of nitrogen across gas/metal contact surface during nitridation is much faster than its dissolution into and/or reaction with the alloy leading to the nitride formation.

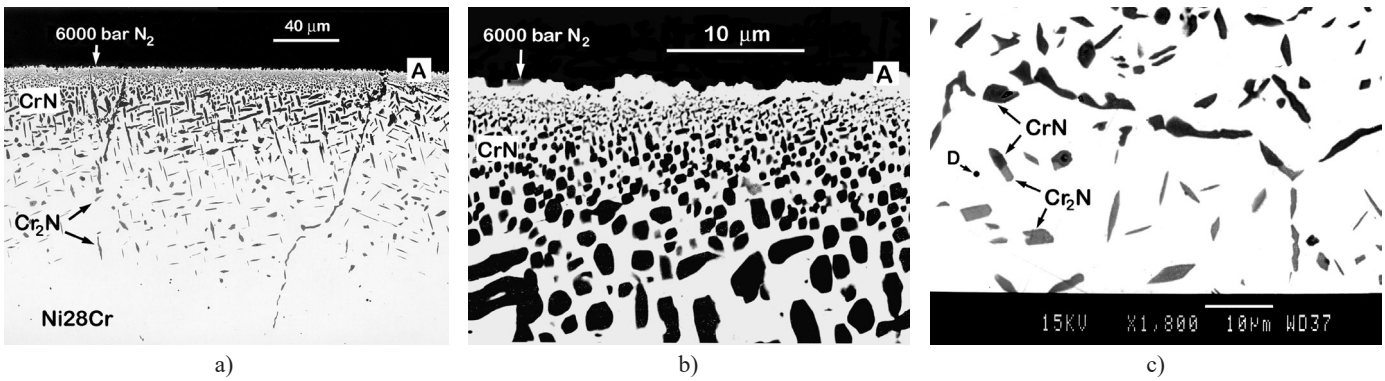

a) b) c)

Fig. 10. Reaction zone microstructure developed Ni28Cr alloy during nitriding at 1125ºC for 4 hours under 6000 bar of N_2-pressure (BEIs): a) general view; b) magnified domain in the vicinity of the metal/gas interface and c) zoomed area of the internally nitride zone showing transition from CrN- to Cr_2N-precipitation. (Letter A indicates the location of the gas/metal interface.)

4.1. Surface nitridation of Ni-Cr alloys

If we assume that equilibrium exists at the gas/metal interface, i.e., the chemical potential (activity) of nitrogen in the alloy at the surface is equal to the chemical potential of nitrogen in the ambient atmosphere, then the reaction products that might form at the alloy surface during nitrogenization can be predicted using thermodynamic stability diagram of the type shown in Fig. 11.

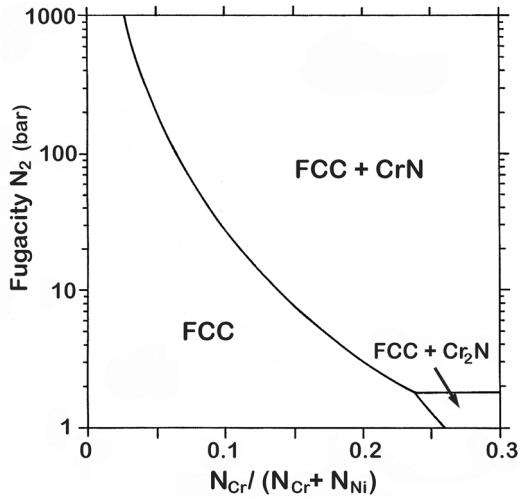

Fig. 11. Calculated thermodynamic stability diagram for chromium nitrides in various Ni-Cr alloys as a function of nitrogen fugacity at 1125ºC. (Note. The "FCC" denotes Ni-based (γ) solid solution with face-centered cubic structure.)

This isothermal construction displays which nitride phases are stable in various Ni-Cr alloys at the specified temperature and external nitrogen fugacity. (Note. The metal ratio $\frac{N_{Cr}}{N_{Cr}+N_{Ni}}$ is chosen in this construction to represent composition because for a fixed value of nitrogen fugacity it varies from *zero* to *unity* as the possible range of alloy compositions is traversed. More details concerning the thermodynamic evaluation and experimental verification of the Ni-Cr-N system can be found elsewhere [17,18].)

To demonstrate application of the stability (potential) diagram, let us return to the results of nitriding experiments carried out under 100 bar of N_2-pressure (Fig. 3a). According to the stability diagram given in Fig. 11, the formation of cubic δ-CrN at 1125ºC and 100 bar of N_2-pressure, is expected only in γ-Ni-Cr solid solution alloys with Cr-content higher than ~6.5 at. %. Indeed, after exposure to these experimental conditions, nitride formation was detected in the Ni-alloy containing 10 at. % of Cr, but not in the Ni-Cr alloy with concentration of Cr only 5 at. %. Clearly, the observed pattern of nitriding behaviour in this system is consistent with the predictions.

To illustrate further the utility of the stability diagrams in rationalizing nitriding reactions, we turn attention to Fig. 5 where microstructure of the internally nitrided zone developed in Ni5Cr alloy after annealing at 1125ºC under 900 bar of N_2-pressure is shown. One can notice from this image that in some locations of the reaction zone (in fact, at the alloy surface), the CrN-particles are in contact (equilibrium) with γ-(Ni-Cr)-based solid-solution matrix and N_2-gas. Such situation can be best seen in Fig. 5b, where a magnified area of the nitrided zone in the vicinity of gas/metal contact surface is shown. The Cr-content in the Ni-based solid solution which equilibrates with cubic δ-CrN and N_2-gas after nitriding under these experimental conditions (1125ºC and 900 bar of N_2-pressure) can be estimated by extrapolating the concentration profile of chromium measured with EPMA across the matrix of the precipitation zone to the metal/gas interface. This value was determined as ~2.8 at. %. The corresponding value for fugacity of N_2-gas in equilibrium with δ-CrN and γ-Ni-based solid solution containing 2.8 at. % of Cr was derived from the thermodynamic assessment of the Ni-Cr-N system as ~1000 bar (Fig. 11). On the other hand, the fugacity of nitrogen at 1125ºC and pressure of 900 bar can be calculated using the Peng-Robinson equation of state [19]. In Fig. 12 the values of the fugacity coefficient, (f/p) as a function of N_2-pressure calculated for different temperatures are presented graphically.

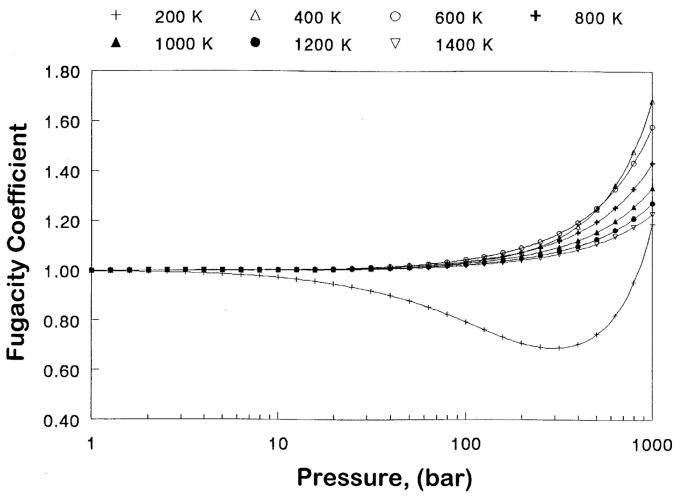

Fig. 12. The variation of fugacity coefficient with pressure for nitrogen gas at different temperatures as calculated with Peng-Robinson equation of state

Using this graph, the nitrogen fugacity, corresponding to 900 bar of N_2 – pressure at 1125ºC was found to be ~1070 bar. One can see that, in general, the thermodynamic predictions agree with the experimental results.

However, one caveat is in order here. The formation of precipitates in a solid matrix is usually accompanied by an increase of net volume. The inevitable consequence of this volume change is matrix deformation around the internal nitride particles precipitated during the internal reaction. The induced stresses are to be relieved in some way [6,10,20-23]. When internal precipitates are relatively coarse and widely spaced, like in the example shown in Figs. 5a, b, the relief of these stresses at relatively high temperatures may occur by plastic flow within the metal grains inside the internal precipitation zone. In such situation, the thermodynamic stability diagrams can indeed be useful in the interpreting surface nitriding. On the other hand,

stress relief may be rather difficult when nitride particles are fine and densely populated.

The type (or combination) of stress relaxation mechanism(s) that may be operational is determined by a number of interrelated factors affecting size, shape and number density of precipitates as well as mechanical properties of the metal matrix inside the internal reaction zone. When internal nitriding of Ni-Cr alloys is carried out under conditions which prevent simultaneous external nitridation, and stress relief, associated with the internal precipitation, occurs by transport (creep) of Ni-based matrix material to the gas/metal interface, resulting in the deposition of a precipitate-free metallic layer at the alloy surface, the proposed thermodynamic approach will not offer the expected predictive capability.

Material deposited by diffusional creep at acceptor boundaries (in the present case, the alloy surface) is observed to be free of any precipitates which may be present in the crystalline grains of the parent material [24-26]. If this material were formed by simple extrusion or dislocation creep, it would be expected to contain internal nitride particles, whereas zones denuded of second phase particles are indicative of diffusional creep. Furthermore, surface dispersion hardening which occurs with internal nitridation would also impede dislocation creep. The definite demarcation between the internal nitride zone and the particle-free surface layer is also indicative of diffusional creep, because the nitride precipitates act as "inert markers", delineating the position of the original alloy surface (e.g., Fig. 9d).

A very telling example of this kind of situation is provided by the results of nitriding experiments conducted at 1125ºC and 6000 bar of N_2-pressure (Figs. 9b, d and Fig. 10b). From the stability diagram (Fig. 11), it follows that in all alloys studied (Ni (5-32) at. % Cr), cubic δ-CrN is expected to be detected at the gas/metal interface. Obviously, this is not the case here. Instead, the formation of a layer of virtually pure nickel, free of nitride particles, was observed on the alloy surface. Clearly, the experimental observations contradict with the predictions made based on the purely thermodynamic grounds.

4.2. Development of internally nitrided zone in the presence of a superficial nitride layer

It is to be recalled, that in reactions between metal alloys and gases, there are, generally, several interrelated factors of importance in determining whether the oxidizable solute (in the alloy) will precipitate internally or form as a continuous layer on the alloy surface [27,28]. Whether exclusively surface reaction or formation of internal precipitates (or combination of both) takes place in the case of gaseous nitriding of Ni-Cr alloys depends on the nitrogen activity in the surrounding atmosphere at the contact surface, the thermodynamic stability of the precipitating compound, i.e., chromium nitride(s), the chemical activity of the solute (Cr) in the initial Ni-based alloy, and also on the relative diffusivities of the penetrating (nitrogen) and solute (Cr) atoms in the γ-Ni(Cr, N)-solid solution.

It was suggested [27] that transition from internal precipitation to exclusive external oxidation should occur when the solute content is sufficient to form a critical volume fraction of internal precipitates at the reaction front. This model is based on the fact that the cross-section available for penetrating element diffusion into the metal phase is reduced owing to the presence of particles of the precipitated compound. As internal precipitates are formed, these virtually impermeable inclusions locally block further reaction between the oxidant and reactive solute because diffusional transport of penetrating species to the reaction front is restricted to the metal channels between those particles which were previously precipitated. This slows the rate at which the supersaturation necessary for new precipitate nucleation can be achieved. In such situation, a sidewise growth of the existing particles (which required a very small supersaturation) rather than the nucleation of new precipitates will occur. If solute content in the initial alloy is high enough to sustain a sufficient (outward) flux needed to maintain growth of precipitates, the particles would grow together and form a compact reaction product layer which would prevent further internal precipitation. Since this elimination of internal precipitation occurs at the very beginning of the interaction, the reaction product layer is formed at the alloy surface.

However, Savva et al. [29] pointed out that since the flux balance decided the volume fraction of precipitates, it is always possible empirically to correlate a critical volume fraction to a change in mode of the reaction (i.e., transition from internal to external oxidation). Based on the results of nitriding experiments with dilute Ni-Ti alloys at 800-1020ºC in nitrogen gas and a nitrogen-argon gas mixture, the authors concluded that blocking has little direct effect on the transition point, i.e., the solute content in the alloy at which the transition from internal precipitation and superficial layer formation takes place. Rather, for a varying interfacial composition, there is an adjustable balance between the inward diffusion of the nitrogen (penetrating species), which favours internal nitridation and the outward diffusion of the solute, which favours a superficial nitride, and this balance becomes unstable at some critical mole fraction of solute in the initial solid-solution alloy. Moreover, diffusion of nitrogen (penetrating element) in transition metal nitrides, like δ-CrN and β-Cr_2N is notable [30], i.e., chromium nitride inclusions are not impermeable for nitrogen.

It seems that the formation of a precipitate-free layer of the γ-(Ni-Cr) solid solution between the superficial layer and the zone of internal precipitation, which can be seen on the micrographs presented in Figs. 1a, b; 4a, b; 6 and 7b, supports the Savva's conclusions. If the mechanism for changing in the nitriding response (i.e., transition from superficial to internal nitride formation) is tied only to the blocking of the Ni-Cr based matrix cross-section by the internal nitride particles, then no "precipitate-free" zone should be expected to appear beneath the surface nitride layer.

Once formed, the surface layer grows slowly by the combination of outward diffusion of chromium from the alloy matrix and inward diffusion of nitrogen through the surface nitride layer.

In this situation, a nitrogen activity inside the alloy is determined by its value at the external nitride layer/alloy interface, rather than at the external surface. Such a reduction of the flux of nitrogen into the material can cause a difference in the precipitation process. For instance, the formation of CrN-precipitates observed in the "corner" of the alloy sample containing 32 at. % of Cr after nitriding at 1125ºC under 100 bar of N_2-pressure (Fig. 4b), is a result of overlapping of fluxes of nitrogen-atoms arriving from the two gas/metal interfaces, which leads to an increasing nitrogen activity inside the alloy.

Formation of a continuous external nitride scale is attending by depletion of chromium from the subsurface-alloy region, which results from the selective nitridation of chromium and the relatively slow diffusion of Cr (compare to that of nitrogen) in the γ-(Ni-Cr) based solid solution. This can be appreciated by looking at, for example, Fig. 13, where a concentration profile for chromium through internal precipitation zone developed in Ni-alloy with 28 at. % Cr after nitriding at 1125ºC and 900 bar of nitrogen for 4 hours is shown. The experimental curve in this figure represents portions of the profile where no interference with nitride particles was encountered.

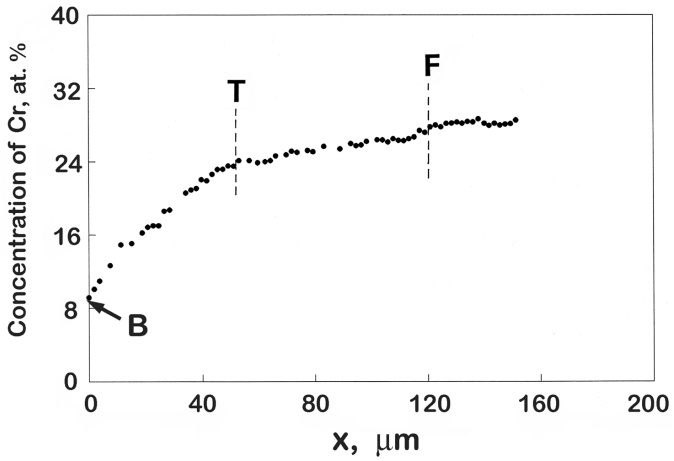

Fig. 13. Concentration profile for chromium through the precipitation internal zone developed after nitriding a Ni-Cr alloy with 28 at. % of Cr at 1125ºC and 900 bar of N_2 for 4 hours. The experimental curve represents portions of the profile where no interference with nitride particles was encountered. (Location in the diffusion zone where transition from CrN- to Cr_2N-precipitation takes place (Fig. 7) is indicated by T, and B and F are the positions of the external nitride/alloy interface and the precipitation front, respectively.)

It is also to be noticed from the concentration profile that, in contrast to the classical cases of internal precipitation reaction [27], in the case at hand, precipitation of the oxidizable solute (Cr) occurs not only at (or in close proximity of) the precipitation front, but continuously through the entire internal nitridation zone.

The simultaneous external and internal nitride formation can be rationalized using a phenomenological approach suggested by Carl Wagner [31]. Suppose that the thermodynamic activity of nitrogen in the two-phase region γ-(Ni-Cr) solid-solution alloy + chromium nitride is determined by the equilibrium $Cr_xN_{(solid)} = xCr_{(alloy)} + [N]_{(alloy)}$. Then, at the interface between the external nitride layer and the alloy where the chromium activity is low, the activity of dissolved nitrogen is greater than in the interior of the Ni-Cr alloy where the activity of chromium is high. Thus, there is a nitrogen activity gradient in the alloy resulting in inward diffusion of nitrogen. Since nitrogen solubility and diffusivity in γ-(Ni-Cr) solid-solution alloy are relatively high, value of the activity product a_{Cr} x a_N beneath the superficial nitride layer/alloy-interface increases with displacement towards the alloy interior. The activity product of nitride (CrN or Cr_2N) is then exceeded at some point, and internal nitride precipitation in the γ-alloy matrix results, while the superficial nitride scale is growing and accordingly the interface between the external nitride layer and the γ-(Ni-Cr) solid-solution alloy is receding.

The curious nature of the nitrogenization process in Ni-Cr-solid solution alloys is also illustrated by the example of the reaction zones containing two different nitride precipitates corresponding to different "oxidation" states, viz. CrN and Cr_2N (Figs. 4b, 7c, d and 10c).

Upon nitridation of Ni-Cr alloys containing 28-32 at. % Cr at 1125ºC and the nitrogen fugacity (activity) sufficiently high allowing for the formation of cubic δ-CrN, the precipitation of the hexagonal β-Cr_2N was found to occur at a certain depth below the alloy surface, where the thermodynamic activity of the inwardly diffusing nitrogen is necessarily lower. The existence of two distinct zones consisting of CrN- and Cr_2N-precipitates is a consequence of the gradient of nitrogen potential between its maximum at the alloy surface, or as in the case when a superficial nitride is formed, the value of nitrogen activity at the external nitride layer/alloy interface, and minimum in the alloy interior.

It is also important to notice that boundary between the two zones of internal precipitates is not sharply defined. This can be explained using a simple thermodynamic consideration. From a purely phenomenological standpoint, the boundary between the two zones of the internal nitrides corresponds to the following reaction:

$$Cr_2N + [N]_d = 2CrN \qquad (1)$$

where $[N]_d$ denotes the diffusing species, i.e., nitrogen.

If the nitrides are pure and stoichiometric, than at a specified temperature, the value of nitrogen activity, a_N, is fixed by the equilibrium corresponding to the conversion reaction expressed by the Eq. (1). In this event, a straight and sharply defined boundary between the zones of δ-CrN- and β-Cr_2N-precipitation is expected to form, providing that local equilibrium prevails in the reaction zone.

It is, however, necessary to realize that the binary chromium nitrides are not stoichiometric ("line") compounds [5]. Moreover, there exists a small solid-state solubility of nickel in the β-Cr_2N-phase [17]. The introduction of the additional component (Ni) in the binary system provides an extra degree of freedom, which allows for the development of not straight and sharply defined (i.e., "wavy") boundary between the CrN- and Cr_2N-precipitation zones even if local thermodynamic equilibria

established and rate of the reaction (Eq. (1)) itself is insignificant in the overall transformation kinetics.

The average Cr-content in the γ-Ni-Cr based solid-solution which is in equilibrium with both cubic δ-CrN- and hexagonal β-Cr_2N-precipitates was measured with EPMA on different samples nitrogenized under external nitrogen pressure 100-6000 bar (Point D in Figs. 4b, 7c and 10c). These values range from 23.8 ± 0.3 to 24.5 ± 0.5 at. %, which is in accordance with the thermodynamic predictions on the position of the three-phase equilibrium γ + δ-CrN + β-Cr_2N in the Ni-Cr-N system. The latter can be seen from Fig. 14 where, for the sake of explanation, two isothermal sections through the Ni-Cr-N phase diagram calculated for 100 and 1000 bar of external nitrogen pressure are presented. (Note. To make these ternary isotherms more readable, a rectangular coordinate system was adopted in these constructions.)

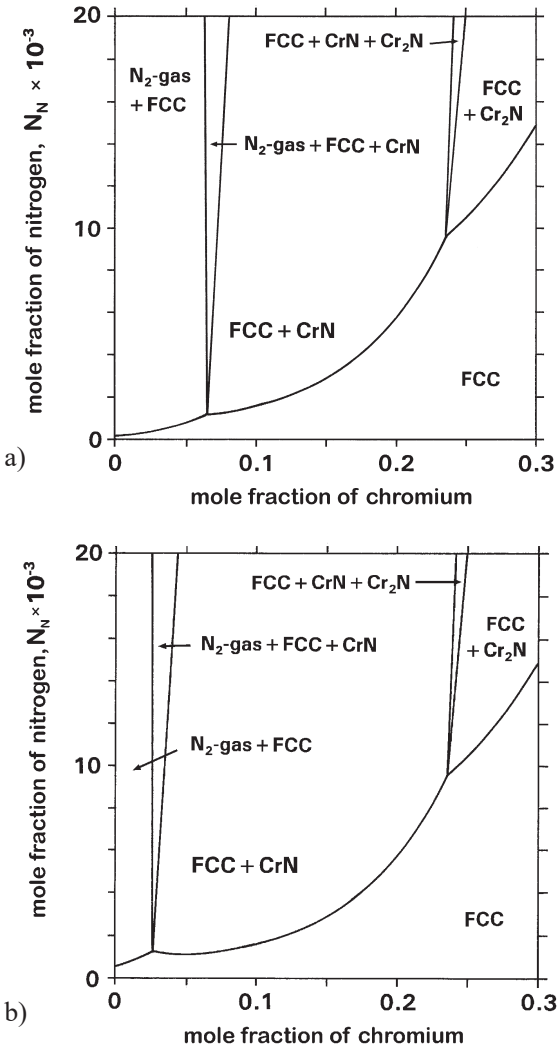

Fig. 14. Calculated isothermal cross-sections through the Ni-Cr-N phase diagram at 1125ºC under various external pressure of nitrogen: a) 100 bar and b) 1000 bar (Note. The "FCC" denotes Ni-based (γ) solid solution with face-centered cubic structure.)

The key feature to note here is that the specified (external) pressure of nitrogen defines the position of the monovariant equilibrium γ + chromium nitride+N_2-gas as well as nitrogen solubility in the γ-(Ni-Cr) based) solid solution. Since the equilibria involving only condensed phases are virtually unaffected by pressure changes in the external gas atmosphere, the rest of the diagram is the same for all pressures.

From the analysis of the isotherms shown in Fig. 14, it follows that with increasing external pressure (fugacity) of nitrogen, the monovariant equilibrium γ + δ-CrN + N_2-gas shifts towards decreasing Cr-content in the γ-phase. The slope of the boundary between the γ and δ-CrN phase fields becomes smaller and even changes sign.

It was also demonstrated in our earlier publications [8,9] that when a moderately stable phase, like chromium nitride(s), is precipitated out during internal precipitation reaction, the distribution of the various species within the diffusion zone can be predicted based on thermodynamic consideration of the respective system. In this case, not only is relative stability of the precipitated compound important, but also the interaction between solute and penetrating atoms in the solid-solution matrix of the precipitation zone must be considered. Nitridation experiments with binary Ni-Cr alloys at 1125ºC gave evidence of "up-hill" diffusion of nitrogen through the Ni-based matrix towards the internal precipitation front. In general, "up-hill" diffusion of the penetrating atoms within the precipitation zone can be predicted from the pertinent phase diagram, since the slope of the boundary of the solid-solution (γ), which is in equilibrium with the internal precipitates is "responsible" for this phenomenon. Since chromium is not precipitated out entirely at the reaction front, nitrogen atoms diffuse in the matrix of the internally nitrided zone not through a nearly pure Ni-lattice but through a solid-solution with a certain concentration of chromium. One might expect that the solubility of nitrogen in the γ-(Ni-Cr) solid solution increases with increasing Cr-content, which can be attributed to the relatively high affinity of chromium to nitrogen. At the isothermal cross-section of the ternary Ni-Cr-N phase diagram (Fig. 14) such situation is reflected by upward solvus curve representing the boundary of the Ni-based solid solution (γ), which is in equilibrium with chromium nitride.

4.3. Formation of ternary π-phase in internally nitrogenized Ni-Cr alloys

Ono et al. [14] reported that the π-phase has the metal-atom arrangement of β-Mn and may be formed in the Ni-Cr-N at 1000ºC through a peritectoid reaction and becomes unstable above 1200ºC. This possibility is confirmed by the reaction zone morphology developed in the Ni32Cr alloy after nitriding at 1125ºC and 1 bar of N_2-pressure followed by slow cooling under 1 bar of N_2. (Fig. 2). A rim of the π-phase around β-Cr_2N-precipitate indicates that a peritectoid reaction between dichromium nitride (β) and the γ-(Ni-Cr) solid solution (i.e., γ + β = π) may occur upon cooling.

After subsequent annealing of such sample at 1125ºC and 1 bar of N_2 and quenching, the π-phase has completely disap-

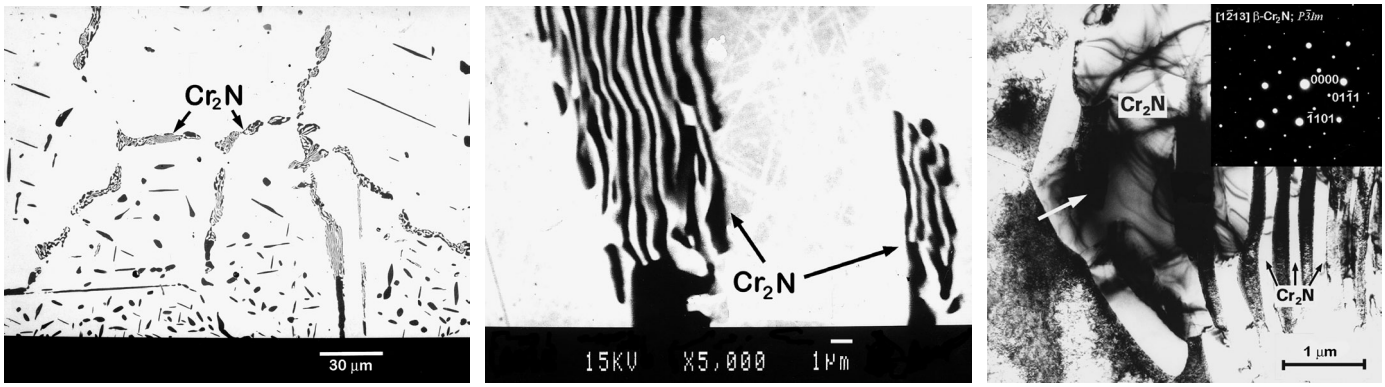

a) b) c)

Fig. 15. Microstructure of the part of internal precipitation zone developed inside Ni32Cr alloy after nitriding at 1125ºC and 1 bar of N_2-pressure for 16 hours followed by a slow cooling under 1 bar of N_2 and subsequent annealing at 1125ºC and 1 bar of nitrogen terminated by quenching: a) general view (BEI) and a magnified area showing lamella morphology of the decomposition product (BEI); c) bright-field (BF) TEM image of the decomposition product along with Selected Area Electron Diffraction Pattern (SAED) taken from the location indicated by arrow and indexed as [1$\bar{2}$13] direction in the hexagonal lattice of β-Cr_2N (P$\bar{3}$1m; a = 0.4811 nm, c = 4484 nm [13])

peared. It has decomposed into lamellar-type structures consisting of γ-phase (Ni-Cr based solid solution) and β-Cr_2N (Fig. 15). This finding substantiates the conclusions of Ono et al. [14].

The present conclusions are also supported by the thermodynamic considerations. In Fig. 16, the calculated stability diagram for the Ni-Cr-N system at 1000ºC is given. (Note. In the thermodynamic assessment used, the π-phase was treated as a compound with a constant metal ratio $\frac{N_{Cr}}{N_{Cr}+N_{Ni}}$.)

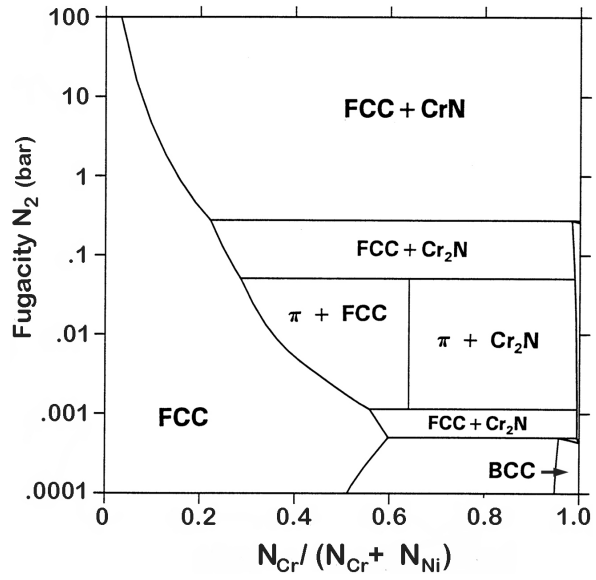

Fig. 16. Thermodynamic stability diagram for nitride phases in various Ni-Cr alloys as a function of nitrogen fugacity at 1000ºC. (The "FCC" and "BCC" designate Ni-based (γ) and Cr-based (α) solid solution with face-centered cubic and body-centered cubic structure, respectively, and π is the ternary phase in the Ni-Cr-N system.)

The thermodynamic analysis demonstrates that at this temperature the π-phase is, indeed, in an equilibrium with γ-(Ni-Cr) based solid solution and β-Cr_2N at modest nitrogen activities. Perhaps, the latter observation may also explain why in the experiments conducted under 1 bar of external N_2-pressure, formation of the π-phase was observed only deep inside the internally nitride zone, but not at the alloy surface. Clearly, our results are in general agreement with the previous findings reported in the literature, although there are some differences in details. The most notable one is that in the work of Ono et al. [14] it was stated that π-phase becomes unstable above 1200ºC. However, we found evidence that this ternary phase decomposes at somewhat lower temperatures, at least, below 1125ºC. Furthermore, the chemical composition of the π-phase was determined by these authors (using EPMA) to be $Cr_{13}Ni_7N_4$, which is slightly different from the results of microprobe measurements performed in the present investigation. Most likely, such a difference can be attributed to the existence of a certain homogeneity range of the ternary π-phase in the Ni-Cr-N system.

5. Concluding remarks

Obviously, the nitridation reactions of Ni-Cr solid-solution alloys can be quite complex. Upon consideration of the experimental results obtained in the present investigation, it becomes apparent that there seems to be an unlimited variety of microstructures which possibly to be developed in the Ni-Cr alloys during gaseous nitriding to the extent that each alloy is almost unique.

Among the variables that may be expected to exercise an influence on the nitriding response of γ-(Ni-Cr) solid-solution alloys to nitrogen atmosphere, the Cr-content in the initial alloy, activity (fugacity) of nitrogen at the gas/metal interface and temperature of nitridation experiment, are the most important.

Reaction behaviour of the Ni-Cr alloy – N_2-gas system can be rationalized (and in some cases even predicted) by using just pertinent thermodynamic information. However, as it was demonstrated, an effect of mechanical stresses induced during the internal precipitation inside the reaction zone can, in some cases, vitiate this prediction. Although little is yet known in a detailed

way of the mechanism of generation and relaxation of these stresses, their manifestations, and their role in the formation of microstructure is evident.

In contrast to the classical cases of internal precipitation reaction, during gaseous nitriding of Ni-Cr alloys at 1125ºC, precipitation of the oxidizable solute (Cr) occurs not only at (or in the close proximity of) the precipitation front, but continuously through the entire internal nitridation zone. In this situation, distribution of various species within the internally nitrided zone can be predicted based on thermodynamic consideration of the respective system. Obviously, in such case, not only is relative stability of the precipitated compound important, but also the interaction between solute and penetrating atoms in the solid-solution matrix of the precipitation zone must be taken into account.

The transition from CrN to Cr_2N precipitation occurs within the reaction zone during nitrogenization at 1125ºC under nitrogen pressure 100-6000 bar when chromium content in the initial alloy is 28 at. % or higher.

It was also observed that a ternary phase, π of the Ni-Cr-N system is formed through a peritectoid reaction between β-Cr_2N and γ-(Ni-Cr) based solid solution inside the nitrided Ni32Cr alloy at 1 bar of N_2 and 1125ºC during cooling from the nitriding temperature.

Perhaps, the attentive reader will find that one important topic, namely nitridation in ammonia, which also falls under the title "gaseous nitriding", is missing in this paper. The authors are fully aware [9,10] of the possibility of creating a high nitrogen fugacity (activity) at the alloy surface by using a flowing ammonia + hydrogen mixture as a nitriding agent. The nitrogen activity at the gas/metal interface generated in this manner can vary in a wide range of values depending on the NH_3:H_2-ratio, temperature and gas-flow rate and can be equivalent with an effective nitrogen pressure of thousands of bars [32,33].

Unfortunately, when a flowing $NH_3 + H_2$ gas-mixture is employed in nitrogenization experiments, the exact value of nitrogen activity (fugacity) imposed on the alloy surface cannot not be defined, which makes any meaningful thermodynamic evaluation of the gas-alloy system impossible. For this reason, the nitridation reactions of Ni-Cr alloys in flowing $NH_3 + H_2$ gas-mixture were not considered in the present work. Instead, the focus here was exclusively on the results of nitriding experiments which have been performed at specified temperature and well-defined pressure (fugacity) of nitrogen.

REFERENCES

[1] A.A. Kodentsov, Diffusion-Controlled Internal Precipitation Reactions, in: A. Paul, S. Divinski, (Eds.), Handbook of Solid-State Diffusion, Elsevier (2017).

[2] A. Kodentsov, Diffusion-limited reactions of non-oxide ceramics with transition metals, in: A. Paul (Ed.), Diffusion Foundations **21**, Trans Tech Publications Ltd (2019).

[3] P. Nash, Bull. Alloy Phase Diagrams **7**, 466-476 (1986).

[4] H.A. Wriedt, N-Ni (Nitrogen-Nickel), in: P. Nash, (Ed.), Phase Diagrams of Binary Nickel Alloys, ASM International, (1990).

[5] M. Venkatraman, J.P. Neumann, in: T.D. Massalski, (Ed.), Binary Alloy Phase Diagrams, ASM International (1991).

[6] S.Y. Chang, U. Krupp, H.-J. Christ, Materials Sci. Eng. A **A301** 196-206 (2001).

[7] R.P. Rubly, D.L. Douglass, Oxid. Met. **35** 259-278 (1991).

[8] A.A. Kodentsov, J.H. Gülpen, Cs. Cserháti, J.K. Kivilahti, F.J.J. van Loo, Metall. Mater. Trans. A **27A**, 59-69 (1996).

[9] A.A. Kodentsov, M.J.H. van Dal, Cs. Cserháti, J.K. Kivilahti, F.J.J. van Loo, Defect Diffusion Forum 143-147, 1619-1624 (1997).

[10] A.A. Kodentsov, M.J.H. van Dal, Cs. Cserháti, L. Daróczi, F.J.J. van Loo, Acta Mater. **47**, 3169-3180 (1999).

[11] F.J. Kedves, L. Gergely, G. Erdélyi, Acta Physica et Chimica Debrecina, 71-85 (1982).

[12] C.A. Wallace, R.C.C. Ward, J. Appl. Cryst. **8**, 255-260 (1975).

[13] JCPDS file No. 35-803, International Center for Diffraction Data, PCPDFWIN v. 2.02, 1999.

[14] N. Ono, M. Kajihara, M. Kikuchi, Met. Trans. A **23A**, 1389-1393 (1992).

[15] JCPDS file No. 77-0047), International Center for Diffraction Data, PCPDFWIN v. 2.02, 1999.

[16] H. Schmalzried, Chemical Kinetics of Solids, VCH Publisher (1995).

[17] K. Frisk, PhD thesis, A Study of the Thermodynamic Properties of the Cr-Fe-Mo-Ni-N System, Royal Institute of Technology, Stockholm, Sweden (1990).

[18] A.A. Kodentsov, M.J.H. van Dal, J.K. Kivilahti, F.J.J. van Loo, Ber. Bunsenges. Phys. Chem. **102**, 1326-1333 (1998).

[19] S.I. Sandler, Chemical and Engineering Thermodynamics, John Wiley & Sons (1999).

[20] J.R. Mackert, R.D. Ringle, C. Fairhurst, J. Dent. Res. **62**, 1229-1235 (1983).

[21] S. Guruswamy, S.M. Park, J.P. Hirth, R.A. Rapp, Oxid. Met. **26**, 77-100 (1986).

[22] H.C. Yi, S.W. Guan, W.W. Smeltzer, A. Petric, Acta Metall. Mater. **42**, 981-990 (1994).

[23] G.C. Savva, G.C. Weatherly, J.S. Kirkaldy, Scripta Mater. **34**, 1087-1093 (1996).

[24] R.L. Squires, R.T. Weiner, M. Phillips, J. Nucl. Mater. **8**, 77-80 (1963).

[25] E.H. Aigeltinger, R.C. Gifkins, Met. Trans. A, **6A**, 2310-2311 (1975).

[26] G.W. Greenwood, H. Jones, T. Sritharan, Phil. Mag. **41**, 871-882 (1980).

[27] C. Wagner, Z. Elektrochem. **63**, 772-790 (1959).

[28] R.A. Rapp, Kinetics, Corrosion **21**, 382-401 (1965).

[29] G.C. Savva, G.C. Weatherly, J.S. Kirkaldy, Metall. Mater. Trans. A **27A**, 1611-1622 (1996).

[30] W. Mayr, W. Lengauer, P. Ettmayer, D. Rafaja, J. Bauer, M. Bohn, J. Phase Equilibria, **20**, 35-44 (1999).

[31] C. Wagner, Corr. Sci. **8**, 889-893 (1968).

[32] M. Katsura, J. Alloys Compd. **182**, 91-102 (1992).

[33] E.J. Mittemeijer, M.A.J. Somers, Surf. Eng. **13**, 483-497 (1997).